DOI: 10.17277/amt.2016.04.pp.011-015

A Giant Increase in the Coercive Force of (PrDy)(CoFe)B Microparticles Ensemble in the Polymer Matrix

R.B. Morgunov[a,b], A.D. Talantsev[a], E.I. Kunitsyna[a]*, V.P. Piskorskii[b], E.N. Kablov[b], O.G. Ospennikova[b]

[a] *Institute of Problems of Chemical Physics, Russian Academy of Sciences, 1, Academician Semenov Ave., Chernogolovka, Moscow region, 142432, Russia*
[b] *Institute of Aviation Materials, 17, Radio Street, Moscow, 105005, Russia*

* Corresponding author: Tel.: +7 (496) 522 19 11. *E-mail*: kunya_kat@mail.ru

Abstract

The (PrDy)(CoFe)B microparticles are the building blocks of sintered magnets. The magnetic properties of (PrDy)(CoFe)B microparticles powder and effects of annealing, fixation of an easy axis on a magnetic hysteresis loop have been analyzed. The fixation of annealed microparticles in a polymer enhances coercive field up to 11 times and energy product up to 6 times. This fact indicates extraction of the true magnetic parameters from magnetic measurements of the powder.

Keywords

Annealing; coercive force; magnetic particles; rare earth metals.

Introduction

Magnetism of the RE-TM-B alloys has been studied in details and attracts huge attention due to unique properties of this new generation of permanent magnets [1 – 3]. Practical application of the NdFeB magnets as well as their modifications obtained by insertion of the Dy, Sm, Pr to rare-earth (**RE**) sublattice and Co to transition metals sublattice (**TM**) is very wide [4, 5]. Industry of permanent magnets is based on technology of sintered magnets. Modification of their properties implies variation of chemical and phase compositions as well as optimization of thermal treatment of alloys. Contributions of multiple factors effect final result determined as coercive field H_c, saturation magnetization M_{sat} and energy product proportional to $M_{sat}H_c$. The presence of the $RE_2TM_{14}B$ main magnetic phase determines quality of magnets. Oxidation, migration of B, replacement of magnetic ions by impurity, change of grain boundary composition, spin-flop transitions and many other processes dramatically change magnetic properties of final sintered magnets in comparison with magnetic properties of the initial building blocks that are RE-TM-B microparticles. Probably, magnetic properties of the microparticles ensemble before sintering are also an important parameter determining quality of the magnets. Nevertheless, no relationship between microparticles powder and sintered magnet has been described in the literature. The problem is absence of the methods for studying magnetic properties of the microparticles ensembles. Magnetic properties of the magnetic powder depend on rotation of the particles in magnetic field, dipole-dipole interaction between them, dry friction and compacting pressure. The influence of these extrinsic factors on magnetic properties of powder devaluates experimental results and does not allow systematic investigation of the relation between magnetic properties of the initial building blocks and sintered magnets. Most of the papers devoted to the studying of permanent magnets present Mossbauer spectra of the initial blocks to discuss properties of the final sintered product. It is explained by the necessity to insert powder in the Mossbauer spectrometer.

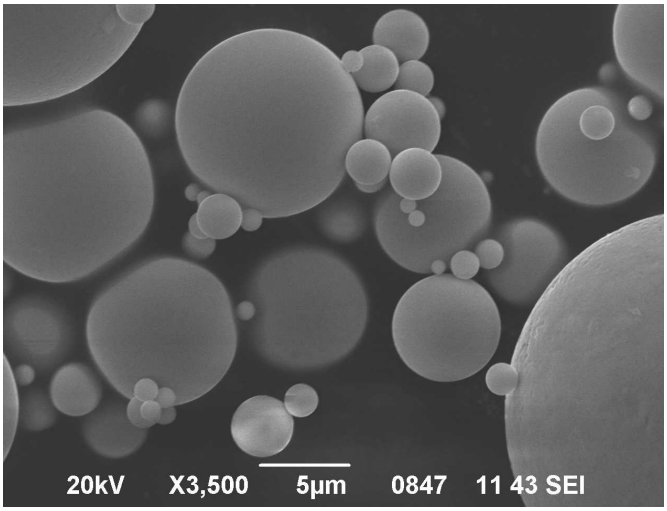

a)

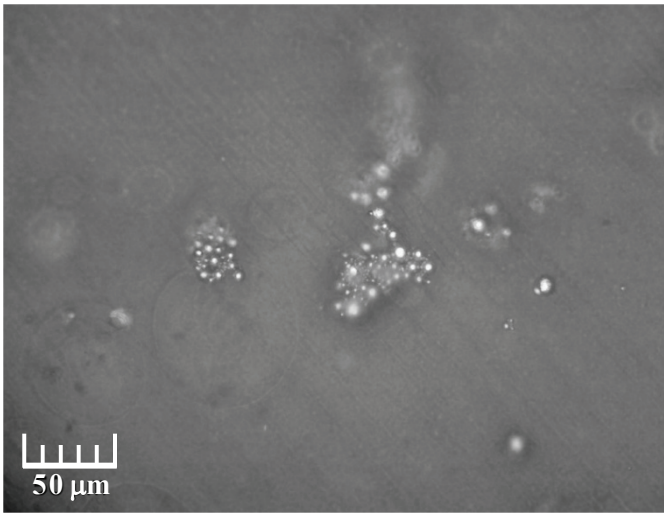

b)

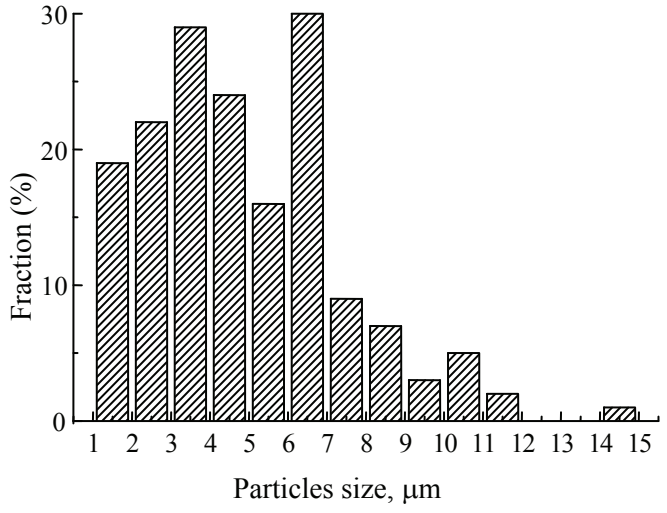

c)

Fig. 1. SEM image of microparticles in "as grown" sample (*a*), photo of the microparticles of the annealed sample, fixed in polymer matrix (*b*), distribution of the microparticles size (*c*)

Ensembles of the magnetic nanoparticles were studied intensively due to their application in magnetic logic [4, 6-7], magnetic hyperthermia [8], and fundamental interest in fractal magnetic systems. Ensemble of hard micromagnetic particles looks like an exotic object in the literature, although applications of the microparticles are wide. The principal difference between nano- and micro-particles is the value of the magnetic moment of the particles increasing up to 10^3 times and resulting in enhancement of magnetic dipole-dipole interactions up to 10^6 times in microparticles. Thus, cooperative effects of particles agglomeration and reorientation of the magnetic moments of individual particles are controlled by strong dipole-dipole interaction, the contribution of which requires experimental study.

Thus, our work was aimed at studying the contributions of fixation of an easy axis in non-magnetic matrix and annealing to magnetic properties of the microparticle ensembles.

Experimental

The alloys were melted in a high-vacuum induction furnace. Argon flow spraying method was used to obtain dispersed melted drops of (PrDy)(CoFe)B crystallized thereafter. Images of the particles obtained with a JSM-840 scanning electron microscope as well as with optical microscopy are presented in Fig. 1 *a*.

Local chemical composition was mapped by electron microprobe analysis using a Superprobe-733 "JCMA-733" microanalyzer (JEOL, Japan). Locality and depth of the analysis were ~1 μm^2 and ~ 1 μm, respectively. Chemical composition was determined from the measurements of line intensity of the secondary X-ray irradiation automatically normalized to the irradiation absorption in the sample. The X-ray spectrum of "as grown" sample shows contributions of 3 crystalline magnetic phases: $(Pr,Dy)_2(Co,Fe)_{14}B$ (phase 2-14-1) was 36 %, $(Pr,Dy)_1(Co,Fe)_4B_1$ (phase 1-4-1) was 32 % and $DyFe_5$ (31 %). The spectrum of the sample after annealing at 900° C shows that contribution of 2-14-1 phase increases up to 92 %, while contribution of 1-4-1 phase decreases down to 8 % and $DyFe_5$ phase disappears.

The "as grown" and annealed samples were studied as free powder, and as fixed particles dispersed in polymer matrix. In free powder the main magnetic axis of the particles follows external magnetic field, whereas the magnetic axes in polymers were fixed chaotically (with no magnetic texturing). Statistical methyl methacrylate co-polymer was used to dissolve magnetic particles and fix their orientations. Mass fraction of the magnetic particles was 10 %. Suspension of the microparticles was obtained by dissolving 0.05 g of polymer in 1 ml of acetone and

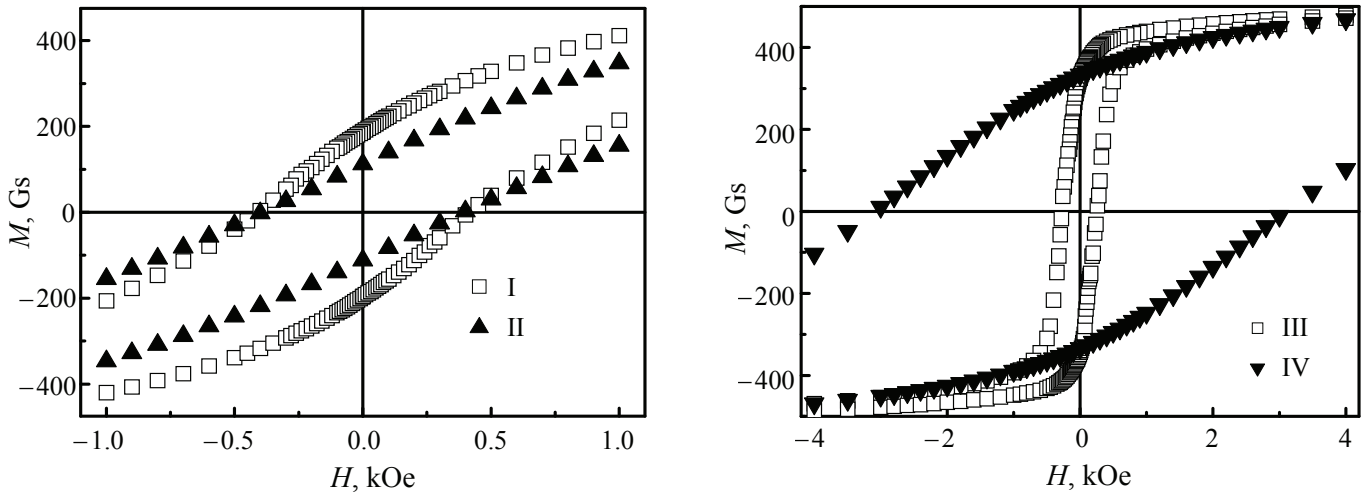

Fig. 2. Dependence of magnetic moment for sample before and after annealing in free powder (I and III) and fixed in polymer matrix (II and IV) on external magnetic field at T = 300 K:
a – before annealing (I and II); *b* – after annealing at T = 900 °C (III and IV).
Dependencies of magnetic induction on magnetic field for the same samples are shown in the inserts

adding microparticles powder. Microparticles were dispersed in polymer using a high-speed rotating rotor (2000 min^{-1} during 20 min). Suspension was deposited on the fluoroplastic substrate and evaporated during 24 hours. The above described process provided films of 200 μm thickness containing homogeneously distributed agglomerates of the microparticles. The images of the microparticles distributed in polymer matrix were obtained by a Neophot 21 microscope equipped with a MYscope 200M digital camera (Fig. 1 *b*). Average diameter of the microparticles was calculated using size distribution of the microparticles (Fig. 1 *c*). Despite the dispersion, agglomeration of the particles was caused by dipole-dipole interaction between them (Fig. 1 *b*). Typical agglomerate contains 50–200 microparticles separated by average distance of ~150 μm.

Magnetization M in constant magnetic field was measured by a superconducting quantum interference device (SQUID) magnetometer (MPMS 5XL Quantum design). The measurements were performed at 300 K in magnetic field H = 0–50 kOe.

Results and Discussion

The comparison of the hysteresis loops of sample before and after annealing is presented in Fig. 2.

Fixation of the magnetic particles in the polymer matrix produces different effects dependently on phase composition of the particles. In the ensemble of "as grown" particles with approximately equal concentrations of the three mentioned above magnetic phases, fixation in polymer does not change coercive field (Fig. 2 *a*) and provides a two-fold decrease of remnant magnetization and magnetic energy product (Table 1). In the ensemble of the annealed particles with dominating 2-14-1 phase, fixation of the particles in the polymer increases coercive field up to 11 times (Fig. 2 *b*) and energy product up to 6 times (Table 1), resulting in magnetic parameters compatible with those typical of $Nd_2Fe_{14}B$ magnet. In our experiments, energy product $(BH)_{MAX}$ of annealed and fixed particles is 2 MG·Oe, while in the $Nd_2Fe_{14}B$ magnets this parameter varies in the range

Table 1

Magnetic parameters of the sample in comparison with sintered $Nd_2Fe_{14}B$

Sample	Remanence B_r, kGs	H_{Ci} (magnetization), Oe	H_C (induction), Oe	$(BH)_{MAX}$, MG·Oe
Free powder before annealing (**I**)	2,3	400	350	0.22
Particles fixed in a polymer before annealing (**II**)	1,4	400	300	0.12
Free powder after annealing(**III**)	4,2	280	260	0.32
Particles fixed in a polymer after annealing (**IV**)	4,2	3000	1900	2
$Nd_2Fe_{14}B$ (sintered) [1]	10–14			21–50

$(BH)_{MAX}$ = 21–50 MG·Oe [2]. This strong effect of particles fixation can be explained. Four factors of the particles remagnetization should be taken into account:

1) remagnetization of each particle limited by domain walls dynamics in the particle;

2) nucleation of the reverse magnetic phase;

3) dipole-dipole magnetic interaction aligning the nearest magnetic moments in opposite directions;

4) dry friction limiting mechanical rotation of the particles.

We will discuss the effect of each mentioned above factor on remagnetization of the ensemble of the magnetic particles for every studied sample.

The presence of 92 % of the main magnetic phase 2-14-1 in the sample after annealing and fixation of the particles in polymer makes it possible to expect magnetic parameters similar with the parameters obtained for the pure RE-TM-B phase described in [9]. Coercive field in the polymer fixed ensemble is controlled by domain walls motion. Critical remagnetization field depends on the number of domains and size of particles [10]. Linear size of the domain w depends on radius of the microparticle r [11]

$$w = (18\ \gamma\mu_0 r)^{1/2}/M_{sat}, \quad (1)$$

γ is the sum of exchange and anisotropy energies normalized on surface area, μ_0 is vacuum magnetic permeability.

Domain width w_C obtained from (1) should be larger than particle diameter $d_C = 2r_C$ to provide the presence of singe domain particles, i.e:

$$2r_C = (18\gamma\mu_0 r_C)^{1/2}/M_{sat},\ r_C = 9\ \gamma\mu_0/2M_{sat}^2. \quad (2)$$

Since critical diameter of $Nd_2Fe_{14}B$ alloys is well known (d_{C0} = 0.2 μm [12–16]), one can estimate the number of domains n in studied microparticles:

$$n = d/w,\ w = d_{C0}\cdot(d/d_{C0})^{1/2} = (d\cdot d_{C0})^{1/2},\ n = (d/d_{C0})^{1/2} \quad (3)$$

The substitution of d = 1–16 μm values in (3) results in n = 2–6. The main part of the studied ensemble is multi-domain particles, the remagnetization of which is provided by magnetic domains. Coercive field of the annealed sample fixed in polymer is 11 times higher than coercive field H_{Ci} = 280 Oe of free powder of the same sample. Freezing of the microparticles rotation in polymer is the only reason for this effect.

In the free powder sample the changes in magnetic axis orientations in the external magnetic field are controlled by dry friction between particles and dipole-dipole interaction between them. The ensemble of unisize microparticles can be considered to estimate contributions of the mentioned factors. The case when external magnetic field **H** is strong enough to orient all microparticle magnetic moments along magnetic field direction **m** ↑↑ **H** will be considered first. Single particle with magnetic moment **m** generates magnetic field in the point characterized by radius-vector **R** ($R > r$):

$$\mathbf{B}(\mathbf{R}) = 3\mathbf{R}(\mathbf{m}\cdot\mathbf{R})/R^5 - \mathbf{m}/R^3. \quad (4)$$

In the plane γ, perpendicular to **m**, magnetic field **B**(**R**) is directed against dipole moment of the microparticles and its value is equal to

$$\mathbf{B}(\mathbf{R}) = -\mathbf{m}/R^3. \quad (5)$$

Magnetic field (5) rapidly decreases as $1/R^3$. For that reason one can neglect interactions with next – nearest neighbors. The distance between microparticles centres is equal to the particle diameter. Therefore, maximal possible number of the neighbour particles in the γ plane is 6, maximal magnetic field induced by neighbour particles is

$$\mathbf{B_{max}} = -6\mathbf{m}/d^3. \quad (6)$$

Substitution of $m = M_{sat}\cdot V$, $V = \pi d^3/6 \approx d^3/2$, d = 8 μm, M_{sat} = 500 Gs results in

$$B_{max} = 3\ M_{sat} = 1500\ \text{Gs}. \quad (7)$$

The torque $\boldsymbol{\tau} = \mathbf{m_2}\times\mathbf{B_{max}}$, rotating particle is maximal if $\mathbf{m_2}\perp\mathbf{B_{max}}$. Field intensity induced by nearest neighbours in point 2, is $|\mathbf{H_{max}}| = |\mathbf{B_{max}}| - 4\pi\cdot M_2$ = 1500 Oe. The above mentioned estimations are convenient if external magnetic field **H** exceeds saturation magnetization of the microparticles ensemble. The decrease of magnetic field **H** below critical value $|H_{max}|$ causes rotation of the particles in the absence of dry friction, i.e. magnetic field H = 1500 Oe should coincide with saturation field of sample magnetization. On the contrary, magnetization curve saturates in magnetic field $H > H_1$ = 2500 Oe. Demagnetization curve demonstrates the decrease of magnetic moment in magnetic field $H < H_2$ = 500 Oe, that is significantly less than 1500 Oe inherent in no friction system.

Experimental $|B_{max}|$ value is between H_1 and H_2 values due to dry friction effect on particle rotation. The torques corresponding to dipole-dipole interaction, dry friction and external magnetic field τ_{dip}, τ_{fr}, τ_H, respectively, should satisfy the following conditions for rotation of the particles:

$$\tau_{dip} - \tau_{fr} \le \tau_H \text{ during magnetization of the ensemble;} \quad (8)$$

$$\tau_{dip} + \tau_{fr} \ge \tau_H \text{ during demagnetization of the ensemble.} \quad (9)$$

Dry friction between particles $\mathbf{f_{fr}}$ is proportional to the area of their surface πd^2. The torque of the friction is proportional to d^3. Thus, correspondent torque is $\tau_{fr} = kd^3/2$, where k is friction coefficient.

The substitution of $\tau_{dip.max} = m \cdot B_{max} = (^3/_2) \cdot M_{sat}^2 d^3$, $\tau_H \sim (^1/_2) M_{sat} \cdot d^3 \cdot H$, $\tau_{fr} - (^1/_2) k d^3$, to (8) and (9) results in:

$$k \le (3M_{sat} - H_2) M_{sat}; \quad (10)$$

$$k \ge (H_1 - 3M_{sat}) M_{sat}. \quad (11)$$

Calculations give

$$k = (3M_{sat} - H_2) M_{sat} = 5 \cdot 10^5 \text{ g} \cdot \text{cm}^{-1} \cdot \text{s}^{-2}.$$

One can obtain for the particles of average size $d_{mean} = 5.5$ μm:

$$\tau_{dip.max} = (^3/_2)\, 2M_{sat}^2 d_{mean}^3 = 6.24 \cdot 10^{-5} \text{ g} \cdot \text{cm}^2 \cdot \text{s}^{-2};$$

$$\tau_{fr} = (^1/_2) k d^3 = 4.16 \cdot 10^{-5} \text{ g} \cdot \text{cm}^2 \cdot \text{s}^{-2};$$

$$\tau_H \le (^1/_2)\, 2M_{sat} d_{mean}^3 \cdot H_1 = 10.4 \cdot 10^{-5} \text{ g} \cdot \text{cm}^2 \cdot \text{s}^{-2};$$

$$\tau_H \ge (^1/_2)\, 2M_{sat} d_{mean}^3 \cdot H_2 = 2.08 \cdot 10^{-5} \text{ g} \cdot \text{cm}^2 \cdot \text{s}^{-2}.$$

These parameters allow one to estimate remnant magnetization of the microparticles ensemble from the given saturation magnetization. In the absence of the external magnetic field the equilibrium state of the ensemble can be determined by equation:

$$\tau_{dip}\,(H = 0) = \tau_{fr},$$

Remnant magnetization is

$$M_{rem} = M_{sat}(\tau_{dip}(H = 0)/\tau_{dip.max}) =$$

$$= M_{sat}(\tau_{fr}/\tau_{dip.max}) = {}^2/_3 M_{sat} = {}^2/_3 \cdot 500 \text{ Gs} = 333 \text{ Gs}.$$

This estimation is in excellent agreement with the experimental value ~335 Gs. Thus, the contribution of dry friction is comparable with dipole-dipole interaction in the ensemble of the annealed particles.

In the ensemble of the "as grown" microparticles containing 36 % of 2-14-1 main magnetic phase, small coercive field H_{Ci} = 400 Oe appears due to domination of the soft magnetic phases, mass fraction of which exceeds 60 %. Coercive field 400 Oe is the same at free and fixed states. It means rotation of microparticles does not contribute to magnetic properties. This can be easily explained in the frame of the model described above. Fixation of the microparticels does not affect coercive field if the condition $|\boldsymbol{\tau_{dip}}| < |\boldsymbol{\tau_{fr}}|$ holds. The decrease in the energy product in the ensemble of the fixed microparticles in comparison with non-fixed system is due to chaotic distribution of magnetic axes of the particles resulting in magnetization of the fraction of particles along their hard axes.

Conclusion

1. The effect of annealing on the shape of magnetic hysteresis loop is different for fixed and free microparticles. Annealing leads to an increase in coercive field H_c for fixed particles and decrease in H_c for non-fixed particles.

2. The coercive field of the ensemble of "as grown" microparticles is controlled by remagnetization of the dominating soft magnetic phases. Fixation of the magnetic axes does not affect the coercive field of the ensemble.

3. The coercive field of non-fixed annealed microparticles is controlled by their rotation in external magnetic field as well as dry friction between the particles and dipole-dipole interaction. The fixation of annealed microparticles in polymer matrix increases coercive field up to 11 times and energy product up to 6 times.

References

1. Khvalkovskiy A.V., Apalkov D., Watts S., Chepulskii R., Beach R.S., Ong A., Tang X., Driskill-Smith A., Butler W.H., Visscher P.B., Lottis D., Chen E., Nikitin V., Krounbi M. Basic principles of STT-MRAM cell operation in memory arrays. J. Phys. D: Appl. Phys., 2013, 46, pp. 074001.

2. Herbst J.F. $R_2Fe_{14}B$ materials: Intrinsic properties and technological aspects. Rev. Mod. Phys., 1991, 63, pp. 819-898.

3. Nishimura N., Hirai T., Koganei A., Ikeda T., Okano K., Seguchi Y., Osada Y. A perpendicular-anisotropy CoFeB–MgO magnetic tunnel junction. J. Appl. Phys., 2002, 91, pp. 5246-5249.

4. Mangin S., Ravelosona D., Katine J.A., Carey M.J., Fullerton E.E. Current-induced magnetization reversal in nanopillars with perpendicular anisotropy. Nature Materials, 2006, 5 pp. 210-215.

5. Albrecht M., Hu G., Moser A., Hellwig O., Terris B.D. Magnetic dot arrays with multiple storage layers. J. Appl. Phys., 2005, 97, pp. 103910.

6. Höink V., Meyners D., Schmalhorst J., Reiss G., Junk D., Engel D., Ehresmann A. Reconfigurable magnetic logic for all basic logic functions produced by ion bombardment induced magnetic patterning. Appl. Phys. Lett., 2007, 91, pp. 162505.

7. Wang J., Meng H., Wang J.-P. Programmable spintronics logic device based on a magnetic tunnel junction element. J. Appl. Phys., 2005, 97, pp. 10D509.

8. Jing Y., Sohn H., Kline T., Victora R.H., Wang J.-P. Experimental and theoretical investigation of cubic FeCo nanoparticles for magnetic hyperthermia. J. Appl. Phys., 2009, 105, pp. 07B305.

9. Poudyal N., Ping Liu J. Advances in nanostructured permanent magnets research. J. Phys. D: Appl. Phys., 2013, 46, pp. 043001.

10. Flávio de Campos M. Trans Tech Publications, Effect of Grain Size on the Coercivity of Sintered NdFeB. Magnets Materials Science Forum, 2010, 660-661, pp. 284-289.

11. Tikadzumi S. Fizika ferromagnetizma: magnitnye characteristic i practicheskie primeneniya [Physics of ferromagnetism: magnetic properties and practical application] Moscow, Mir, 1987. 222 p. (Rus).

12. Girt Er., Krishnan K.M., Thomas G., Girt E., Altounian Z. Coercivity limits and mechanism in nanocomposite Nd–Fe–B alloys. J. Magn. Magn. Mater., 2001, 231, pp. 219-230.

13. Chen W., Gao R.W., Zhu M.G., Pan W., Li W., Li X.M., Han G.B., Feng W.C., Wang B. Magnetic properties and coercivity mechanism of isotropic HDDR NdFeB bonded magnets with Co and Dy addition. J. Magn. Magn. Mater., 2003, 261, pp. 222-227.

14. Kronmuller H., Fahnle M. Micromagnetism and the microstructure of Ferromagnetic solids. Cambridge University Press, Cambridge. 2003. Chapter 6, p. 120.

15. Serrona L.K.E.B., Fujisaki R., Sugimura A., Okuda T., Adachi N., Ohsato N., Sakamoto I., Nakanishi A., Motokawa M., Ping D.H., Hono K. Enhanced magnetic properties of Nd–Fe–B thin films crystallized by heat treatment. J. Magn. Magn. Mater., 2003, 260, pp. 406-414.

16. Lu B., Huang M.Q., Chen Q., Ma B.M., Laughlin D.E. Magnetic coupling in boron-rich NeFeB nanocomposites. J. Appl. Phys., 1999, 85, pp. 5920-5922.